Journal of Rock Mechanics and Geotechnical Engineering 14 (2022) 329–345

Contents lists available at ScienceDirect

Journal of Rock Mechanics and Geotechnical Engineering

journal homepage: www.jrmge.cn

Full Length Article

A novel approach to structural anisotropy classification for jointed rock masses using theoretical rock quality designation formulation adjusted to joint spacing

Harun Sonmez*, Murat Ercanoglu, Gulseren Dagdelenler

Applied Geology Division, Geological Engineering Department, Faculty of Engineering, Hacettepe University, Beytepe, Ankara, 06800, Turkey

ARTICLE INFO

Article history:
Received 24 February 2021
Received in revised form
21 July 2021
Accepted 19 August 2021
Available online 1 November 2021

Keywords:
Anisotropy index of jointing degree
Anisotropy of rock mass
Rock mass classification
Jointing degree
Theoretical rock quality designation

ABSTRACT

Rock quality designation (*RQD*) has been considered as a one-dimensional jointing degree property since it should be determined by measuring the core lengths obtained from drilling. Anisotropy index of jointing degree (AI_{jd}) was formulated by Zheng et al. (2018) by considering maximum and minimum values of *RQD* for a jointed rock medium in three-dimensional space. In accordance with spacing terminology by ISRM (1981), defining the jointing degree for the rock masses composed of extremely closely spaced joints as well as for the rock masses including widely to extremely widely spaced joints is practically impossible because of the use of 10 cm as a threshold value in the conventional form of *RQD*. To overcome this limitation, theoretical *RQD* ($TRQD_t$) introduced by Priest and Hudson (1976) can be taken into consideration only when the statistical distribution of discontinuity spacing has a negative exponential distribution. Anisotropy index of the jointing degree was improved using $TRQD_t$ which was adjusted to wider joint spacing by considering Priest (1993)'s recommendation on the use of variable threshold value (t) in $TRQD_t$ formulation. After applications of the improved anisotropy index of a jointing degree (AI'_{jd}) to hypothetical jointed rock mass cases, the effect of persistency of joints on structural anisotropy of rock mass was introduced to the improved AI'_{jd} formulation by considering the ratings of persistency of joints as proposed by Bieniawski (1989)'s rock mass rating (RMR) classification. Two real cases were assessed in the stratified marl and the columnar basalt using the weighted anisotropy index of jointing degree ($W\_AI'_{jd}$). A structural anisotropy classification was developed using the *RQD* classification proposed by Deere (1963). The proposed methodology is capable of defining the structural anisotropy of a rock mass including joint pattern from extremely closely to extremely widely spaced joints.

1. Introduction

It is generally known that both strength and deformability of rock mass may change with joint geometry and arrangement (Cheng et al., 2016). Structural anisotropic behavior may be significant in rock mass volume depending on number of sets, orientation, spacing and persistency characteristics of the joints. As an evident example, the strength and deformation properties of the stratified rock masses may have significant differences in parallel and perpendicular directions to the stratification planes. The effect of joints on the anisotropic behavior of a jointed rock mass, such as the compressive strength, shear strength and failure pattern, needs to be evaluated as part of safety assessments for any rock engineering project (Wang et al., 2017). Rock masses are usually located in jointed heterogeneous media, encompassing two types of elements such as rock blocks and joints (Sow et al., 2017). Jiang et al. (2014) investigated mechanical anisotropy of columnar jointed basalts by laboratory and in situ tests. They emphasized that mechanical anisotropy must be considered when assigning input parameters for various classification and numerical analysis schemes. Due to the new technological developments of geo-spatial measurements, researchers have focused on the studies about the determination of three-dimensional (3D) joint distribution using these high-tech equipments such as terrestrial light detection and ranging (LIDAR) technique and unmanned aerial vehicle (UAV)

* Corresponding author.
E-mail address: haruns@hacettepe.edu.tr (H. Sonmez).
Peer review under responsibility of Institute of Rock and Soil Mechanics, Chinese Academy of Sciences.

https://doi.org/10.1016/j.jrmge.2021.08.009

photogrammetry (Riquelme et al., 2015; Wichmann et al., 2019; Kong et al., 2020, 2021). A classification, the anisotropic rock mass rating (ARMR) similar to rock mass rating (RMR), was proposed by Saroglou et al. (2019) for rating of anisotropic rock mass. They aimed to determine ARMR score that could be an input for the geomechanical calculations rather than assessing the structural anisotropy depending on directional jointing degree.

For safe, applicable and economic designs of a rock engineering project to be constructed in/on a rock medium is almost impossible without considering the quantified geological parameters. Engineering design parameters of the rock masses have been derived by considering the quantified values of both intact rock and joint properties. The strength and deformation parameters of intact rock are generally obtained by laboratory studies employed on rock core samples. However, properties of joints considering their origin such as bedding, jointing or faulting should be defined in the field by expert's observations and measurements. On the other hand, rock quality designation (*RQD*) has been considered as a valuable parameter for defining the one-dimensional (1D) jointing degree in addition to core recoveries such as total core recovery (TCR) and solid core recovery (SCR). Measurement of *RQD* can be directly conducted by core drilling studies or can be indirectly determined by scanline surveys on rock mass exposures.

While large number of studies are available about the use of *RQD* for determination of strength and deformation parameters of rock masses (Coon and Merritt, 1970; Gardner, 1987; Kulhawy and Goodman, 1987; Gokceoglu et al., 2003; Kayabasi et al., 2003; Zhang and Einstein, 2004; Zhang, 2010), *RQD* has also been used as one of the input parameters in rock mass classification systems such as RMR, Q and geological strength index (GSI) (Bieniawski, 1989; Barton, 2002; Dinc et al., 2011; Hoek et al., 2013; Bertuzzi et al., 2016) and for improvement of the existing classification systems (Sen and Sadagah, 2003; Zheng et al., 2016). In addition to these valuable studies by rock engineering aspect, core recovery parameters including *RQD* are considered as important parameters for estimation of mineral resources as given by Annels and Dominy (2003). The measurement of *RQD* from surface to depth is considered as a standard parameter of core logging for the site investigation. Therefore, *RQD* can be evaluated as a valuable quantity to be used in different disciplines such as engineering rock mechanics, engineering geology and even mineral resource exploration. The average value of *RQD* is generally considered in engineering geology and rock engineering projects by the expert decision. However, *RQD* is a directional property by measuring of core length in drilling or joint spaces in scanline on rock mass exposure. In addition to the investigations about the directivity of *RQD* in the literature (e.g. Choi and Park, 2004; Palmström, 2005; Zheng et al., 2018), a recent numerical definition of directivity of *RQD* was used by Zheng et al. (2018).

In this study, anisotropy index equation developed by Zheng et al. (2018) was improved to overcome limitations on the use of its original form to the rock masses with spacing of joints ranging from extremely close to extremely wide ones. As stated by Zheng et al. (2018), drillings in vertical direction are abundant when compared with horizontal and few inclined drills. Therefore, collecting of joint data and the values of *RQD* in 3D space is difficult and expensive using conventional *RQD* procedure performed on drill cores. Theoretical *RQD* ($TRQD_t$) formulation proposed by Priest and Hudson (1976) can be used as a powerful solution to overcome this difficulty. However, it should be remembered that $TRQD_t$ equation introduced by Priest and Hudson (1976) can be taken into consideration only when the statistical distribution of discontinuity spacing has a negative exponential distribution. For this aim, the formulation of anisotropy index of jointing degree (AI_{jd}) proposed by Zheng et al. (2018) and the $TRQD_t$ by Priest and Hudson (1976) were combined. In addition to this improvement, a new structural anisotropy classification for rock mass was developed. Then, a structural anisotropy chart based on new structural anisotropy classification was presented.

Furthermore, the formulation proposed in this study for evaluation of structural anisotropy of rock mass with its classification has a potential to be introduced to serving as one of the input parameters in any anisotropic geomechanical rock mass classifications such as ARMR.

Table 1
Description of rock mass quality based on *RQD* (Deere, 1963).

RQD (%)	Description
0–25	Very poor (VP)
25–50	Poor (P)
50–75	Fair (F)
75–90	Good (G)
90–100	Excellent (E)

2. Brief history of *RQD* and anisotropy index of jointing degree (AI_{jd})

The fundamental studies about the development of the *RQD* date back to 1960s (Deere, 1963, 1968; Deere et al., 1967). *RQD* has been an indispensable input parameter in many rock engineering applications since its introduction. *RQD* and its classification were introduced as a quantity for defining quality of the rock masses (Table 1). It could be divided into five classes and its range changes from 0% to 100%.

The valuable discussions about the measurement of *RQD* such as core diameter and length of coring run were well documented by Deere and Deere (1989). Threshold length of rock core was accepted as 10 cm in the conventional procedure for defining the rock mass structure. Although *RQD* was valuable quantity about jointing degree of rock masses, extensive studies related to the limitations of the use of *RQD* were also available in the literature. For example, Palmström (2005) indicated that "*similar to all types of 1-dimensional measurements (boreholes and scanlines), RQD is directional, but due to its definition, it is more sensitive to the hole or line direction than joint spacing or fracture frequency measurements*". Although directivity of *RQD* might be mentioned as a limitation of *RQD* for defining jointing degree in 3D space, it may also be evaluated as an advantage for defining structural anisotropy of rock mass due to its directivity property, which was first reported by Zheng et al. (2018). As widely discussed in the literature, the use of *RQD* alone has not been preferred in rock mechanics due to its limitation, it has also been preferred as one of the input parameters in well-known rock mass classification systems such as RMR, Q and quantified GSI (Bieniawski, 1989; Barton, 2002; Dinc et al., 2011; Hoek et al., 2013). The relations between volumetric joint count (J_v) and *RQD* depending on the block shape have been investigated in the literature (Sen and Eissa, 1991; Palmström, 1995; 2005). Recently, Zheng et al. (2020) performed a study on the relation between J_v and *RQD* in 3D space.

As a well-known expression by practitioners, *RQD* is a ratio of total length of rock core pieces equal to or longer than 10 cm to the total length of run in a drilling operation. Although most of the drill holes are conducted in vertical direction, oriented drill holes are also possible for measuring the core parameters. However, it is not commonly possible to perform drilling in many different directions due to the time-consuming procedures and cost. Therefore, assessment of the anisotropic behavior of the rock mass structure by considering the value of *RQD* as a directional parameter requires exhaustive efforts in terms of time and expenses. However, an

alternative theoretical relation was also established for determination of *RQD* from measurements obtained from scanline surveys. Priest and Hudson (1976) derived a theoretical equation between the average frequency of joints and the value of $TRQD_t$ based on inserting the limit "*t*" as a threshold level. In the $TRQD_t$ equation given in Eq. (1a), frequency of joints (λ) can be easily obtained from average spacing of joints (S) measured in scanline surveys. Priest and Hudson (1976) derived the $TRQD_t$ equation by assuming that the statistical distribution of discontinuity spacing has a negative exponential distribution.

$$TRQD_t(\%) = 100e^{-t\lambda}(t\lambda + 1) \quad (1a)$$

$$\lambda = 1/S \quad (1b)$$

where λ is the frequency of joints in m^{-1}, and S is the average spacing of joints measured in m.

Wu et al. (2021) published a very valuable paper about the advances in statistical mechanics of rock masses. In their study, *RQD* distribution in 3D space was determined using $TRQD_t$ formulation with the threshold level of 0.1 m proposed by Sen (1984). However, the proposed formulation by Sen (1984) considers that the statistical distribution of joint spacing is exponential. The relation proposed by Sen (1984) may also be used for determination of *RQD* based on average joint spacing. But, in this study, the formulation derived by Priest and Hudson (1976) is preferred because of the wide use of this relation in rock mechanics. On the other hand, any $TRQD_t$ relation based on different statistical distributions may be adapted easily to the methodology presented in the rest part of our study.

Priest (1993) indicated that the conventional *RQD* with the threshold level of $t = 0.1$ m gives *RQD* that is sensitive to mean spacing up to only approximately 0.3 m, while *RQD* increases by only 5% in response to increase in mean spacing beyond this value (Fig. 1).

As seen in Fig. 1, *RQD* has not sufficient capability for identifying the degree of jointing for extremely closely rock jointed masses and also from widely to extremely widely jointed rock masses in accordance with spacing terminology by ISRM (1981). An improvement in sensitivity of *RQD* to higher values of mean spacing can be achieved by increasing the threshold level as emphasized by Priest (1993). The use of 0.1 m as a threshold value in conventional *RQD* procedure may be accepted as a sufficient threshold value for defining quality of rock mass in terms of strength and deformability assessments. By considering Priest (1993)'s impressive comment about the use of higher threshold levels in determining the theoretical *RQD* to improve its sensitivity, the limitation of the use of conventional *RQD* procedure to define jointing degree for the rock mass having spacing of joints from wide to extremely wide was overcome. For this aim, variable threshold level was used depending on the widest spaced joint set to satisfy $TRQD_t$ as the possible upper quantity of ~99%. Firstly, the mean (average) joint spacing was determined depending on the values of threshold level (t) from 0.1 to 2 to satisfy $TRQD_t$ as 99% (Fig. 2a). Then, a curve type relation between the lowest frequency of joint sets in a direction of 3D rock mass medium (λ_{1_mass}) and threshold level "*t*" was obtained (Fig. 2b). In other words, λ_{1_mass} can also be defined as the lowest value of the directional joint frequency representing with trend/

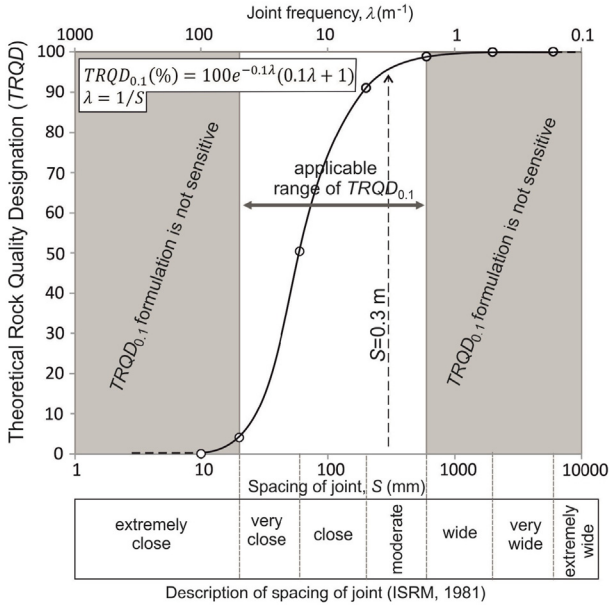

Fig. 1. Applicable range of $TRQD_{0.1}$ and its relation with description of spacing of joints suggested by ISRM (1981).

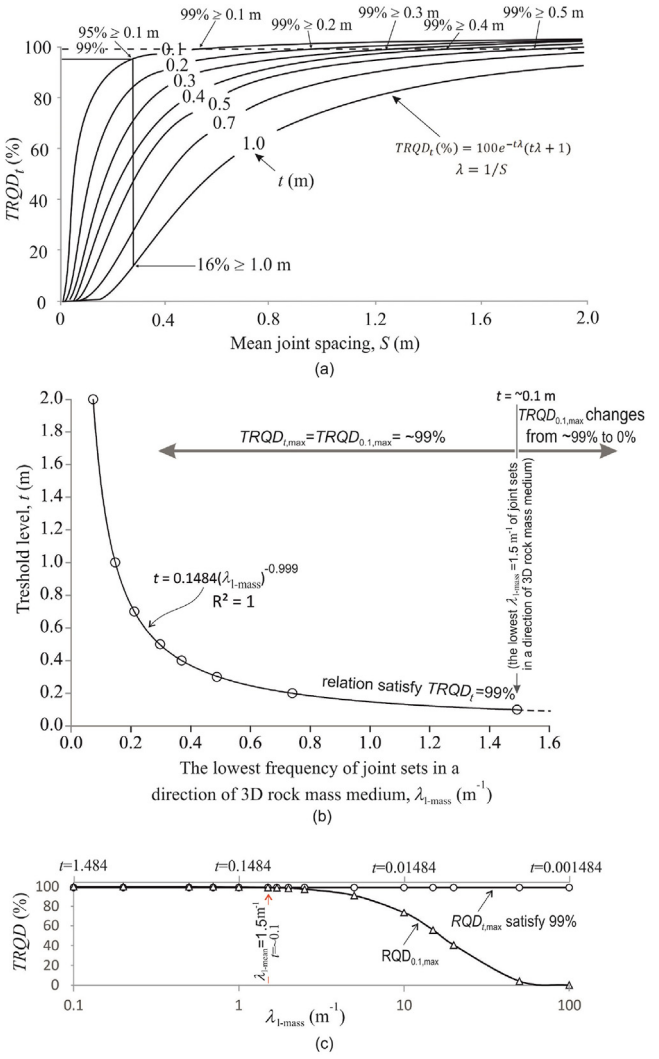

Fig. 2. (a) Variation of $TRQD_t$ with mean joint spacing for a range of $TRQD_t$ threshold values "*t*" (modified after Priest and Hudson, 1976), (b) Relation between the lowest frequency of joint sets in a direction of 3D rock mass medium ($\lambda_{1\text{-mass}}$) and threshold level "*t*" to satisfy $TRQD_t$ as 99%, and (c) Graphical presentation of $TRQD_{0.1,max}$ and $TRQD_{t,max}$ with the value of $\lambda_{1\text{-mass}}$.

plunge in 3D rock mass medium. Graphical presentation of $TRQD_{0.1,max}$ and $TRQD_{t,max}$ with the value of (λ_{l_mass}) is given in Fig. 2c, where $TRQD_{0.1,max}$ is the maximum value of theoretical *RQD* when $t = 0.1$ m.

Although structural anisotropy of the rock mass is directly related to the block shape, it should be improved as an identifying index value to extend its applicability to the rock masses having joints from extremely closely to extremely widely spaced joints. For this aim, the size (spacing of joints) dependency of $TRQD_t$ was standardized considering the widest spaced joint set in 3D space to satisfy $TRQD_t$ as 99% (Fig. 2). Threshold value "*t*" can be calculated by Eq. (2) based on the lowest frequency of joint sets in a direction of 3D rock mass medium ($\lambda_{l\text{-}mass}$) to satisfy $TRQD_{t,max} = 99\%$.

$$t = 0.1484(\lambda_{l\_mass})^{-0.999} \tag{2}$$

As discussed before, the value of *RQD* is highly sensitive to the directivity particularly for highly anisotropic rock masses since *RQD* is a 1D quantity. Therefore, it should be underlined that *RQD* may change in different directions depending on the degree of structural anisotropy of the rock masses. The most of the rock masses in nature are anisotropic and the directivity of *RQD* exactly reflects the anisotropic characteristic of an actual rock mass (Zheng et al., 2018).

The studies on determination of joint frequency and/or *RQD* depending on direction and its variation in 3D space have been an attractive topic in rock mechanics literature (Choi and Park, 2004; Zheng et al., 2018). Basically, the studies about the variations of *RQD* in 3D space were investigated based on the determination of joint frequency (λ) (Eq. (1a)) depending on the orientation of the scanlines.

As mentioned by Karzulovic and Goodman (1985) and Hudson and Priest (1983), Eq. (3) can be taken into consideration for determination of joint frequency (λ) along a specific scanline orientation by considering the values of each joint set in a rock mass:

$$\lambda = \sum_{i=1}^{N} \lambda_i \cos\theta_i \tag{3}$$

where N is the number of joint sets, λ_i is the true (normal to joint set) frequency of ith joint set, and θ_i is the angle between direction of scanline and normal to joint set. However, there can be some discrepancies or biases for this assumption and practice due to random fractures (Choi and Park, 2004). However, the random joints may not be highly related for assessment of structural anisotropic behavior of a rock mass.

Eqs. (1)–(3) can be used together for determination of *TRQD* along a specific direction from the scanline measurements for specific threshold level "*t*". As stated by Zheng et al. (2018), application of this approach requires more number of scanlines or boreholes with cored (M) than number of joint sets (N). Since the M value is larger than N, Zheng et al. (2018) suggested the adaptation of the minimizing quadratic error approach proposed by Karzulovic and Goodman (1985) to calculate the 1D densities of the joint sets in the normal directions for larger number of M than N. However, the joints of each joint set were assumed fully parallel to each other and randomly oriented joints in rock masses were not taken into consideration.

Due to its nature, rock masses commonly include non-perfectly parallel joints even if they belong to the same joint set. In addition, the size of joints in a rock mass volume may be limited. Zheng et al. (2018) tried to develop a relation for determination of the joint frequency depending on 1D direction including the normal (perpendicular) directions of the joint sets by considering non-perfectly parallel joints with the limited sizes. Since this concept is out of the scope of this study, for more detailed calculation steps, readers are referred to Zheng et al. (2018).

The use of equal-angle stereographic projection of lower hemisphere was practically preferred for the presentation for the distribution of *RQD* in 3D-space (Choi and Park, 2004; Zheng et al., 2018). Although the angular definition of a point on equal-angle stereographic projection is given by the values of trend and plunge, it is also possible to define the same point by using formulation in x and y Cartesian coordinate system of equal-angle stereographic projection based on the lower hemisphere (Eq. (4a) and (4b)). An illustration of a total of 360 points on the equal-angle stereographic projection net using 10° increments (in both trend from 000° to 350° and plunge from 0° to 90°) was used in this study. The sensitivity of the calculations can be increased by reducing 10° increments used for both trend and plunge values on equal-angle stereographic projection. However, 10° increments were considered as sufficient to reflect the directivity changes of the quantities such as λ or $TRQD_t$ in this study. Any directional property such as $TRQD_t$ is assigned to all defined points on the equal-angle stereographic projection net, and can be contoured using x, y and property values (Priest, 1993).

$$x = R\cos\alpha\tan\left(\frac{90^\circ - \beta}{2}\right) \tag{4a}$$

$$y = R\sin\alpha\tan\left(\frac{90^\circ - \beta}{2}\right) \tag{4b}$$

where R is the radius of lower hemisphere equal-angle projection and the orientation of a line is defined by trend (α) and plunge (β) in degree.

As mentioned above, a point on equal-angle stereographic projection defines the direction of a line by its trend and plunge, normal to the orientation of joint surface as a 1D property. In accordance with the discussed methodology herein, *RQD* can be illustrated by the practitioners on the equal-angle stereographic projection using a direction of a line by its trend and plunge. By considering *RQD* counters on equal-angle stereographic projection, the possible minimum and maximum values of *RQD* (RQD_{min} and RQD_{max}) can also be determined in 3D rock mass medium.

Wu et al. (2021) defined structural anisotropy index as a ratio of RQD_{min} to RQD_{max}. This simple ratio can be used for defining structural anisotropy of rock mass based on degree of jointing. However, this ratio has limited capacity in some cases to define structural anisotropy depending on the value of RQD_{max}. For example, both $RQD_{max} = 100\%$ and 10% yield $RQD_{min}/RQD_{max} = 0$ when $RQD_{min} = 0$. Similarly, let us select some combinations of RQD_{max} and RQD_{min} having differences between each RQD_{max} and RQD_{min} pairs of 10% (such as 100%–90%, 90%–80%, …, 20%–10% and 10%–0%). For these cases, the values of structural anisotropy index as a ratio of RQD_{min} to RQD_{max} change from 0.9 to 0. In other words, it is not clear that change from 0.9 to 0 of structural anisotropy index is acceptable when the difference between RQD_{min} and RQD_{max} is only 10%.

The increase in structural anisotropic behavior of rock mass in terms of engineering aspects could be expected when the difference between RQD_{max} and RQD_{min} also increases. By considering this fact, Zheng et al. (2018) defined an anisotropy index of jointing degree (AI_{jd}) by

$$AI_{jd} = \frac{RQD_{max}}{100}(RQD_{max} - RQD_{min}) \tag{5}$$

As mentioned by Zheng et al. (2018), the values of RQD are

obtained as the same in all different directions when $RQD_{max} = RQD_{min}$ with $AI_{jd} = 0$. On the other hand, when $RQD_{max} = 100$ and $RQD_{min} = 0$, then $AI_{jd} = 100$ is obtained as an upper bound of structural anisotropic value.

In this study, the relation given in Eq. (5) was improved by replacing RQD with $TRQD_t$ to define an index value to overcome limitation of the conventional RQD procedure for identifying jointing degree of the rock masses having particularly widely and extremely widely spaced joints (Eq. (5)). On the other hand, the impact of the anisotropy may be expected less for extremely closely jointed rock masses. To reduce the anisotropic behavior of densely jointed rock masses, the ratio of $TRQD_{0.1,max}$ to 100 is taken into consideration as a reduction multiplier in the improved AI_{jd} equation, given in Eq. (6). On the other hand, $TRQD_{0.1,max} = 99\%$ will be used for rock mass including widely to extremely widely spaced joints due to the assumption explained in Fig. 2. Hence, the effect of multiplier will be negligible for these cases. As a result, while the original AI_{jd} formulation is preserved, an improvement is introduced to AI_{jd} formulation by Eq. (5) in order to extend its applicability capacity for rock masses composed of extremely small to extremely large rock blocks. After the proposed improvement, increase in the sensitivity of the $\Delta TRQD_t$, which equals to difference between $TRQD_{t,max}$ and $TRQD_{t,min}$, is now considered as possible using threshold level "t" representing with the lowest frequency of joint sets in a direction of 3D rock mass medium ($\lambda_{1\text{-mass}}$) lower than 1.5 m^{-1} in extremely widely spaced joints. Some additional assessments were also investigated by hypothetical cases of certain block shapes under the related part of the study.

(a) Combination matrix between $TRQD_{t,max}$ and $TRQD_{t,min}$ together with proposal of AI'_{jd} classes

$TRQD_{t,max}$ \ $TRQD_{t,min}$	Very Poor (VP)	Poor (P)	Fair (F)	Good (G)	Excellent (E)
Excellent	H	M	L	VL	NO
Good	M	L	VL	NO	X
Fair	L	VL	NO	X	X
Poor	VL	NO	X	X	X
Very Poor	NO	X	X	X	X

Proposed AI'_{jd} classes: VH: Very High anisotropy, H: High anisotropy, M: Moderate anisotropy, L: Low anisotropy, NO: No Anisotropy, X: not applicable combination.

$$AI'_{jd} = \frac{TRQD_{0.1,max}}{100}\left(TRQD_{t,max} - TRQD_{t,min}\right)$$

$TRQD_{t,max} = TRQD_{0.1,max}$ case is considered

(b)

$TRQD_{t,max}$ \ AI'_{jd}	VP (RQD_{mid}=12.5)	P (RQD_{mid}=37.5)	F (RQD_{mid}=62.5%)	G (RQD_{mid}=82.5%)	E (RQD_{mid}=95%)
E (RQD_{mid}=95%)	78.4	54.6	30.9	11.9	0
G (RQD_{mid}=82.5%)	57.8	37.1	16.5	0	X
F (RQD_{mid}=62.5%)	31.3	15.6	0	X	X
P (RQD_{mid}=37.5%)	9.4	0	X	X	X
VP (RQD_{mid}=12.5%)	0	X	X	X	X

(c) Determination of boundary values of AI'_{jd} for each classes

AI'_{jd_max}: 100 (for upper bound)	I	→ 89.2
average AI'_{jd} for H: 78.4	II	→ 67.3
for M: 56.2 =(57.8+54.6)/2	III	→ 44.7
for L: 33.1 =(31.3+37.1+30.9)/3	IV	→ 23.3
for VL: 13.4 =(9.4+15.6+16.5+11.9)/4	V	→ 6.7
AI'_{jd_min}: 0 (for lower bound)	VI	

(d) Structural anisotropy index classification of AI'_{jd}

Description	Symbol	AI'_{jd}
I: Very High	VH	90 - 100
II: High	H	65 - 90
III: Moderate	M	45 - 65
IV: Low	L	25 - 45
V: Very Low	VL	5 - 25
VI: Almost No Anisotropy	~NO	0 - 5

Fig. 3. The followed steps for the development of the improved structural anisotropy index of jointing degree (AI'_{jd}) classification.

$$AI'_{jd} = \frac{TRQD_{0.1,max}}{100}\left(TRQD_{t,max} - TRQD_{t,min}\right) \quad (6)$$

where AI'_{jd} is the improved formulation of anisotropy index of jointing degree. While AI'_{jd} varies between 0 and 100, the higher values of AI'_{jd} reflect the stronger structural anisotropy of jointing degree of a rock mass.

Definition of the values of AI'_{jd} using a standardized classification such as the known classifications of numerous index parameters used in rock engineering will be better to improve the practical value of AI'_{jd} in terms of rock engineering applications. Additionally, it will be helpful for communication among the related disciplines.

3. Development of *TRQD*-based structural anisotropy index classification of rock masses

In this study, a classification for structural anisotropy index of jointing degree was developed using the engineering classification of *RQD* (Table 1) which is widely accepted by rock engineering community (Deere et al., 1967).

For this aim, the following steps were followed for determination of the boundary values of AI'_{jd} for each class in a new structural anisotropy index classification of rock masses:

(1) Combination matrix of the classes based on $TRQD_{t,min}$ and $TRQD_{t,max}$ is prepared by considering the five *RQD* classes given in Table 1. While combination of "Excellent" and "Very poor" is named "Very high (VH)" anisotropy, combinations of same class pairs such as "Excellent" versus "Excellent" or similarly "Poor" versus "Poor" were named "Almost no anisotropy (~NO)" (Fig. 3a). Other combinations were named within these two boundary conditions by considering the degree of anisotropy with difference of *RQD* classes in the combinations (Fig. 3a).

(2) Middle values of $TRQD_{t,min}$ and $TRQD_{t,max}$ for five classes presented in Table 1 from "Excellent" to "Very poor" and AI'_{jd} equation (Eq. (6)) were used together for determination of each combination of the defined anisotropy classes (Fig. 3b).

(3) Average values of AI'_{jd} for boundaries of each anisotropy class from "Very high (VH)" to "Very poor (VP)" were calculated using determination listed in Fig. 3b. In addition, $AI'_{jd} = 100$ and 0 were considered as upper and lower bounds for "Very high (VH)" and "Almost no anisotropy (~NO)", respectively (Fig. 3a).

(4) As given in Fig. 3d, structural anisotropy index classifications composed of five classes from "Very high (VH)" to "Almost no anisotropy (~NO)" with the boundary values of AI'_{jd} were suggested by considering the values listed in Fig. 3c.

4. Applications to hypothetical and real cases

Applications of new structural anisotropy index classification to hypothetic and real cases were presented in this section. Firstly, the

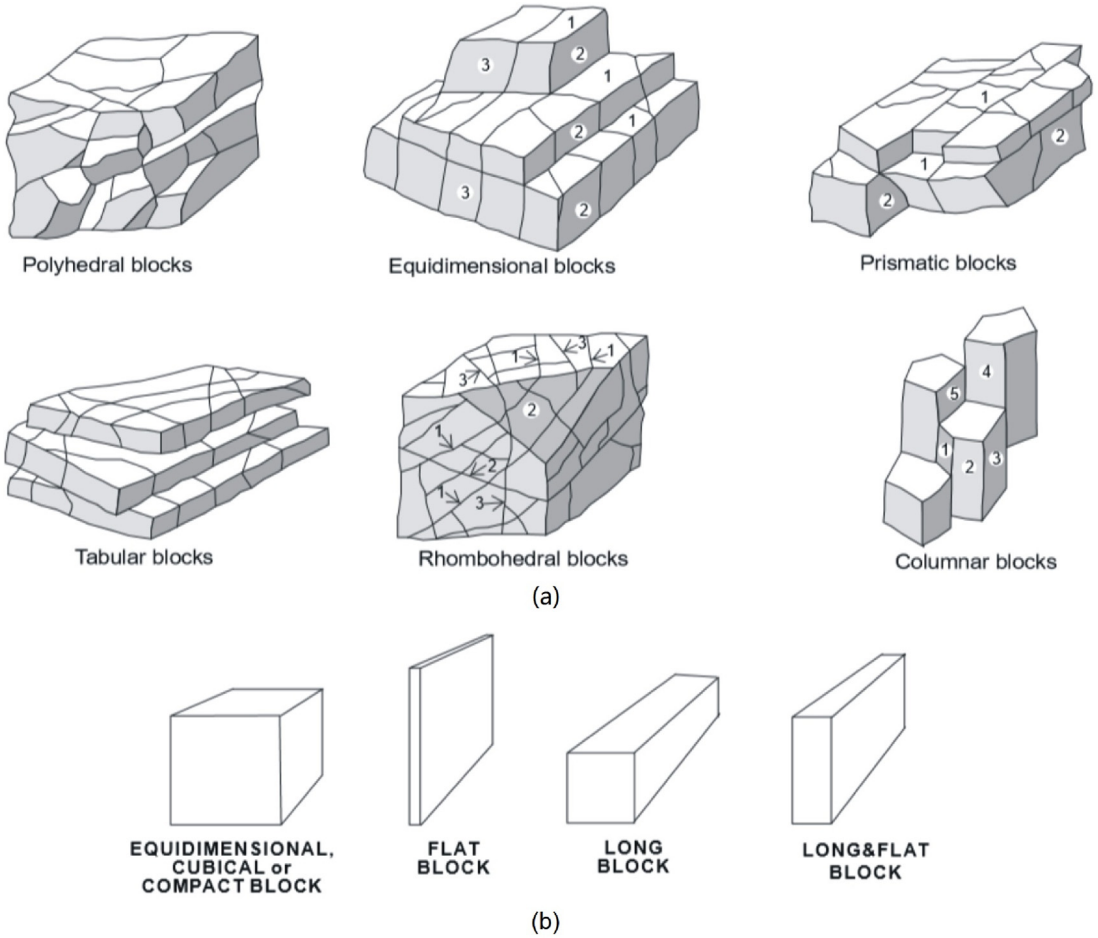

Fig. 4. (a) Examples of the block shapes and joint patterns identified by Dearman (1991), and (b) Block shapes of rock masses including three joint sets used by Palmström (2000).

use of new structural anisotropy index classification by considering hypothetical cases of some certain block shapes was investigated. Then, its application to the real cases was presented.

4.1. Hypothetic cases of some certain block shapes

At the first stage, the hypothetic cases were preferred to apply the structural anisotropy index classification to rock masses composed of some certain block shapes. Both original (AI_{jd}, considering conventional threshold level as $t = 0.1$ m) and the improved formulation (AI'_{jd}) of anisotropy index of jointing degree were used together for comparison of applicability of the proposed procedure to the rock masses including closely and widely spaced joints.

Examples of the block shapes and joint patterns identified by Dearman (1991), and block shapes of rock masses including three joint sets used by Palmström (2000) are represented in Fig. 4. In this stage of the study, the main block shapes illustrated in Fig. 4b were assessed using the formulations of the anisotropy index and the proposed structural anisotropy index classification. For this aim, the

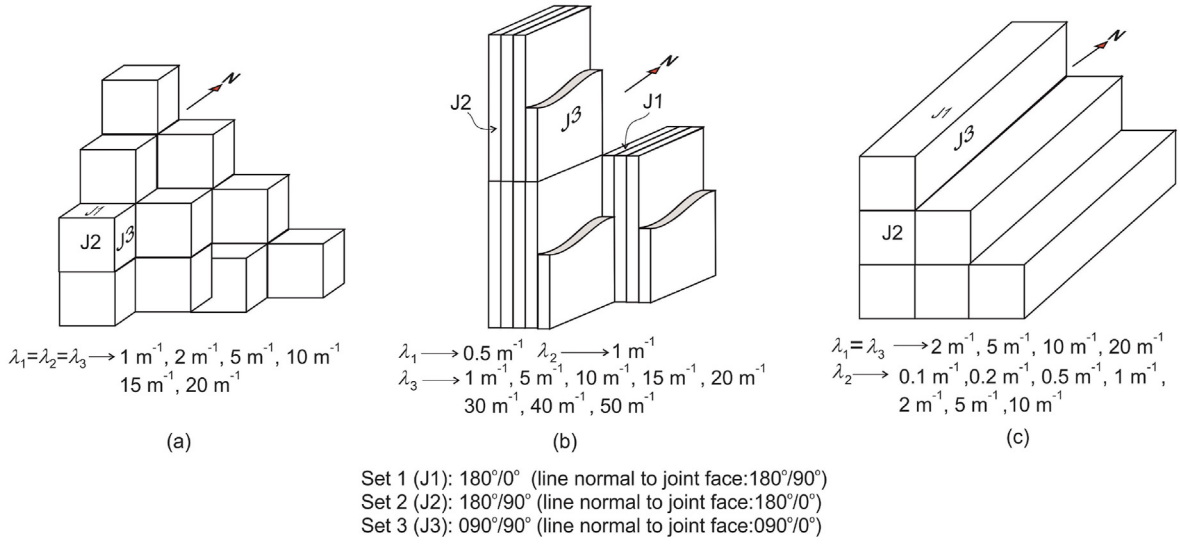

Fig. 5. The values of joint frequencies (λ) for each set used in the hypothetical assessment of anisotropy index classification for (a) cubic, (b) flat and (c) square based long block shapes composed of three joint sets.

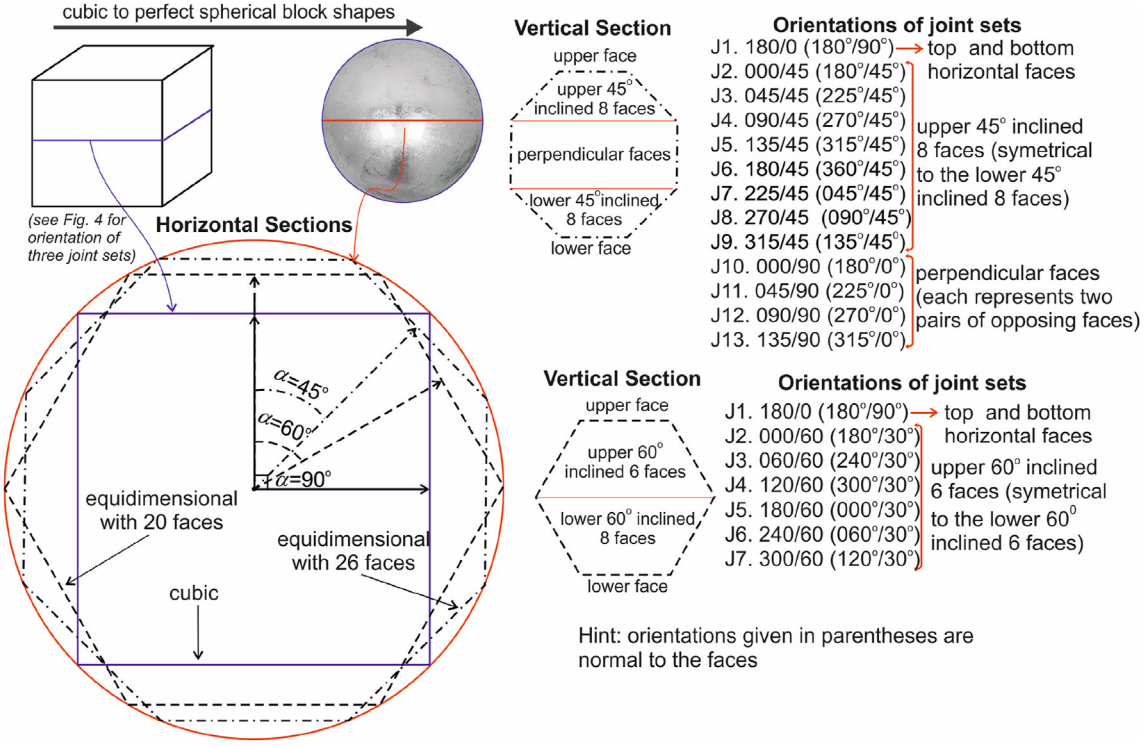

Fig. 6. Definition of joint (face) orientations for equidimensional cubic block shapes with 6 faces ($\alpha = 90°$ between faces which represent joint surfaces), for equidimensional blocks with 26 faces ($\alpha = 45°$ between faces which represent joint surfaces) and for equidimensional blocks with 14 faces ($\alpha = 60°$ between faces which represent joint surfaces) towards hypothetical perfect spherical block shape.

joint frequencies for each set in each hypothetic rock mass were varied from lower values to higher values to define possible effects of block size in the proposed anisotropy index classification (Fig. 5).

In the first hypothetic case (H-case-1), in addition to equidimensional cubic block shapes with 6 faces ($\alpha = 90°$ between faces which represent joint surfaces), equidimensional blocks with 26 faces ($\alpha = 45°$ between faces which represent joint surfaces) and 14 faces ($\alpha = 60°$ between faces which represent joint surfaces) towards hypothetical perfect spherical block shape were also investigated (Figs. 5a and 6).

As seen in Fig. 7a, the high AI_{jd} value was obtained for cubic block shape when λ is equal to $\sim 10\ m^{-1}$, and it is classified as very low anisotropy (VL) in the proposed structural anisotropy index classification. The value of AI_{jd} decreases on both sides from $\lambda = \sim 10\ m^{-1}$ because of the limitations on the use of *RQD* for rock masses composed of extremely closely and extremely widely spaced joint sets for higher and lower λ values. In other words, the difference between RQD_{max} and RQD_{min} reduces to zero due to limitations on the use of *RQD* for rock masses composed of extremely closely and extremely widely spaced joint sets. In addition, RQD_{max} increases up to 100% for the lower value of λ. Similarly, the value of RQD_{max} reduces towards zero for the higher λ values.

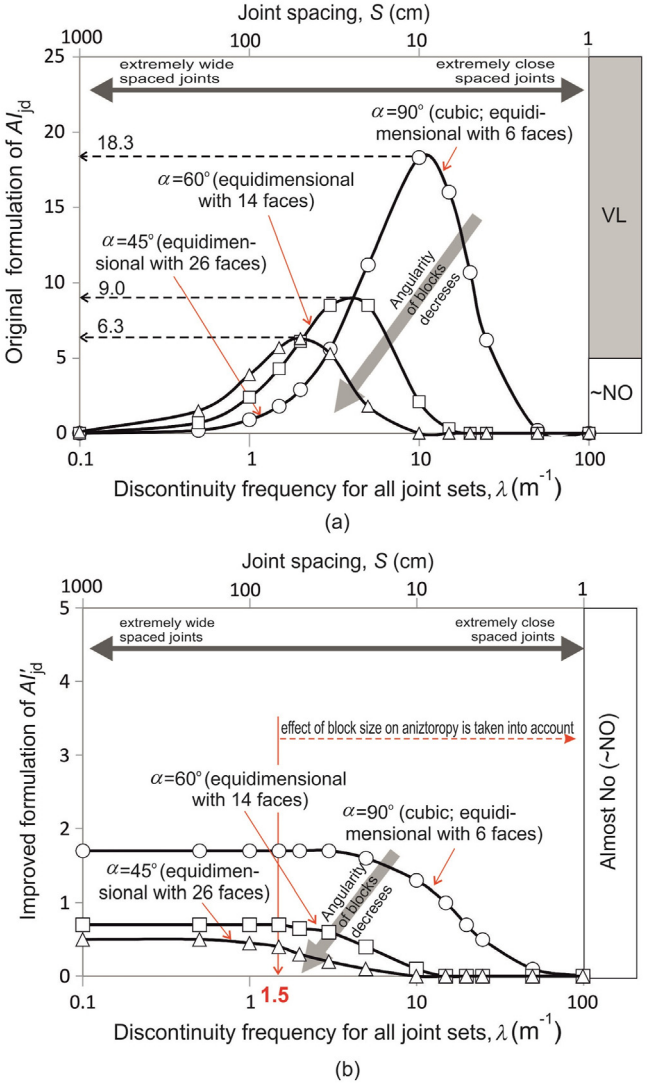

Fig. 7. The relations among (a) original (AI_{jd}) and (b) the improved (AI'_{jd}) formulations of anisotropy index of jointing degree with joint frequency (λ) defined as the same for all joint sets in three cases of equidimensional cubic block shapes with 6 faces, equidimensional blocks with 26 faces and equidimensional blocks with 14 faces.

The distributions of $TRQD_{0.1}$ and $TRQD_t$ for every possible direction on equal-angle stereographic projection were determined using the procedures explained in detail before depending on trends between 0° to 350° for every 10° increments and for plunges from 0° to 90° for every 10° increments. As seen in plotting of all directions by trend and plunge on equal-angle stereographic projection, totally 360 groups of $TRQD_{0.1}$ and $TRQD_t$ were determined depending on the changes in trend and plunge. The variations of original (AI_{jd}) and improved (AI'_{jd}) formulations of the anisotropy index of jointing degree depending on joint frequencies of equidimensional blocks having $\alpha = 90°$, 60° and 45° between faces are given in Fig. 7.

The other important outcome of the assessment of H-case-1 is that the small AI_{jd} values are obtained for block shapes which move towards perfect equidimensional spherical shape due to the increase in number of joint sets of the block. This situation is an expected result of increasing roundness with an increasing number of joint sets. Theoretically, the value of AI_{jd} converges to zero for perfect spherical shape. While the decrease in the value of AI_{jd} can be considered as meaningful to a certain extent for extremely closely jointed rock masses, such an assessment is completely out of question for rock masses having widely to extremely widely spaced joint sets. However, the original formulation of AI_{jd} given by Eq. (5) is not capable of overcoming this limitation particularly for rock masses composed of widely to extremely widely spaced joint sets. This situation is clearly observed in Fig. 7a. When the block shape is remained, the values of AI_{jd} decrease for lower λ values because of the use of conventional *RQD* ($= TRQD_{0.1}$) equation which is defined for threshold level of $t = 0.1$ m. The improved formulation of anisotropy index of jointing degree (AI'_{jd}) successfully overcomes this situation as seen in Fig. 7b. While the block size (or spacing of joints) effect on anisotropy is considered for λ higher than 1.5 m^{-1}, AI'_{jd} is remained constant for λ less than 1.5 m^{-1} (Fig. 7b).

When the original AI_{jd} formulation is considered, the anisotropy class of the three cases having equidimensional shapes in 3D space is classified from very low anisotropy (VL) to almost no anisotropy (~NO) depending on higher number of joint sets. On the other hand, the improved formulation of AI'_{jd} produces lower values which are classified as almost no (~NO) from cubic shapes to more rounded block shapes having higher number of joint sets. In a rock engineering point of view, the anisotropic behavior is not expected for blocks having equidimensional shapes. Therefore, the improved formulation of AI'_{jd} seems more meaningful for identifying anisotropic class of rock masses in a wide structural range from heavily jointed rock mass to extremely widely spaced rock mass. As an illustration for *TRQD* evaluation of rock masses having about widely spaced joint sets, the $TRQD_t$ distribution curves on equal-angle stereographic projection for each subcase of equidimensional block shapes having $\lambda = 1.5\ m^{-1}$ are given in Fig. 8.

The second hypothetic case (H-case-2) is investigated on block shapes changing from columnar to flat (Fig. 4b). For this aim, a square based ($\lambda_1 = \lambda_2$) block shape was transformed from columnar into flat using different values of λ_3 as the third dimension. Five different dimensions for square based block from very large ($\lambda_1 = \lambda_2 = 0.1\ m^{-1}$) to very small ($\lambda_1 = \lambda_2 = 50\ m^{-1}$) were investigated by considering original and improved formulations of structural anisotropy index denoted by AI_{jd} and AI'_{jd}. The third dimension of spacing of joint (S_3) was selected as very high value of $S_3 = 1000$ m that is equal to $\lambda_3 = 0.001\ m^{-1}$ to obtain columnar block shape and it was reduced to very small value such as lamination dimension of $S_3 = 0.001$ m, equal to $\lambda_3 = 1000\ m^{-1}$.

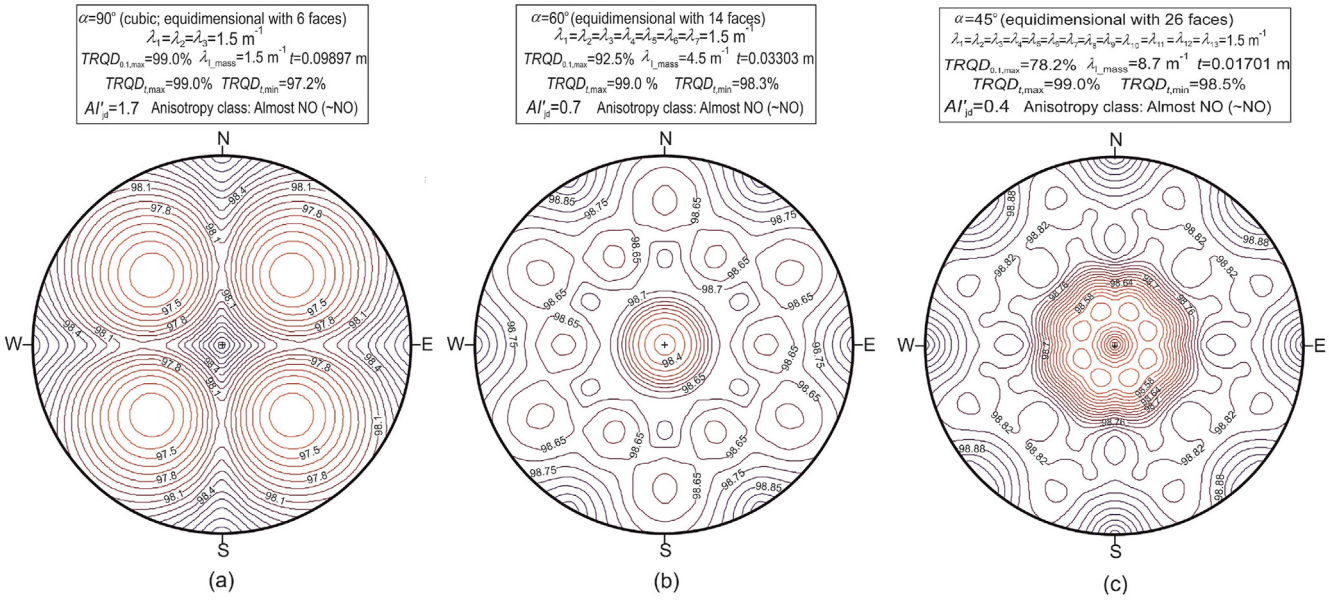

Fig. 8. $TRQD_t$ distribution curves on equal-angle stereographic projection for each subcase of equidimensional block shapes having the value of $\lambda = 1.5\ m^{-1}$ from cubic shape towards perfect equidimensional spherical shape: (a) $\alpha = 90°$, (b) $\alpha = 60°$ and (c) $\alpha = 45°$.

As seen in Fig. 9a, the original formulation (AI_{jd}) is insufficient for identifying degree of anisotropy for the cases which represents rock mass models having about widely and extremely closely spaced joint sets due to the applicable range of $TRQD_{0.1}$ between 99% and 1% for $\lambda_3 < 1.4\ m^{-1}$ ($S_3 > 0.7$ m) and for $\lambda_3 > 66.7\ m^{-1}$ ($S_3 < 0.015$ m), respectively.

On the other hand, while the values of AI_{jd} starts from almost zero for the cases having larger base dimensions such as $S_{1,2} = 5$ m and 1 m, the values of AI_{jd} starts from almost 100 for the cases having smaller base dimensions such as $S_{1,2} = 0.02$ m because of the applicable ranges of $TRQD_{0.1}$. Therefore, the capacity of the original structural anisotropy index is limited when the whole range of possible joint spaces are taken into consideration.

It should be expected that structural anisotropy should be increased while moving towards two opposite directions from the peak value of AI_{jd} such as towards columnar or flat shapes from equidimensional cubic block shape by changing the third dimension. In addition, the modeled rock mass having cubic block shape should be classified as almost no anisotropy at the center (Fig. 9b). As explained before, in the improved formulation of AI'_{jd} and its classification, the 3D block size effects on structural anisotropy can be taken into consideration for rock masses including widely spaced joints with λ higher than $1.5\ m^{-1}$. Therefore, the possible maximum anisotropy index values towards smaller block sizes reduce to lower values than 100 such as the modeled rock masses having $\lambda_1 = \lambda_2 = 4\ m^{-1}$, $20\ m^{-1}$ and $50\ m^{-1}$ (Fig. 9). Two examples of $TRQD_t$ distribution curves on equal-angle stereographic projection for columnar and flat sub-cases are given in Fig. 10.

The following outcomes can be drawn from the results of the assessment of hypothetic cases on the proposed anisotropy index classification:

(1) The limitations of the use of traditional *RQD* with threshold value "*t*" equal to 0.1 is overcome both for the rock masses composed of extremely closely spaced joints and for the rock mass including spacing of joints from widely to extremely widely by the improved formulation of AI'_{jd} and the proposed anisotropy index classification. However, anisotropic effects on the behavior of rock mass may be expected insignificant

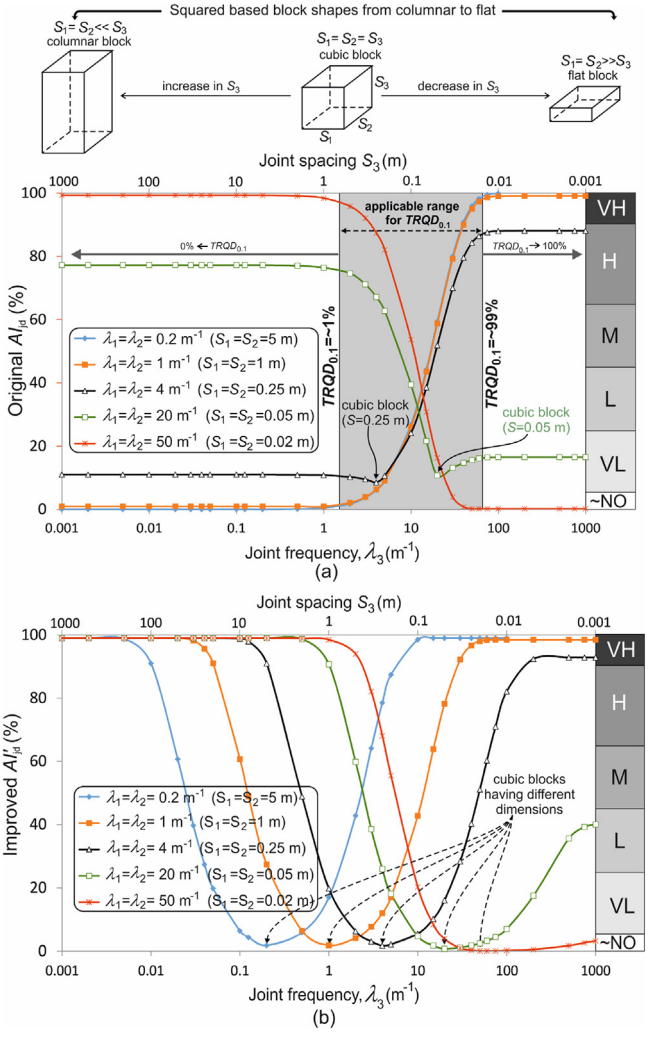

Fig. 9. The values of (a) AI_{jd} and (b) AI'_{jd} depending on third joint frequency (λ_3) of square based ($\lambda_1 = \lambda_2$) block shape from columnar to flat block.

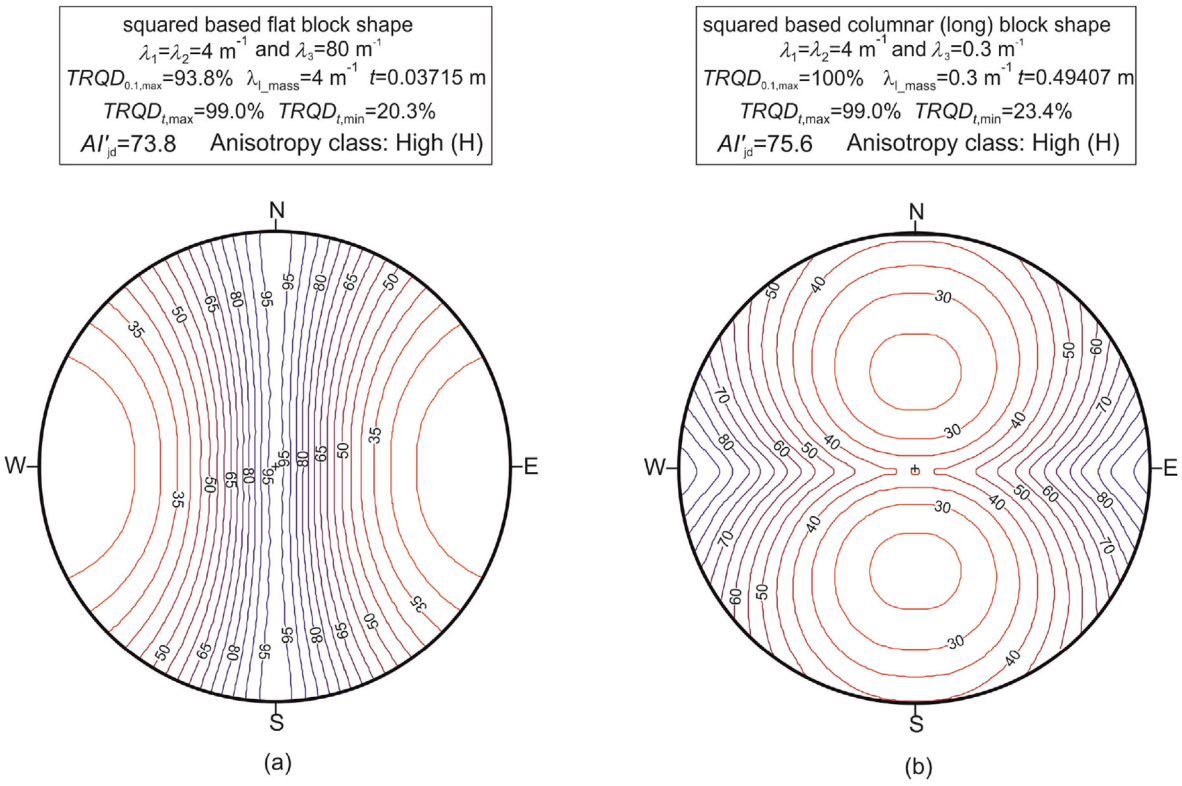

Fig. 10. $TRQD_t$ distribution curves on equal-angle stereographic projection for (a) flat block shapes ($\lambda_1 = \lambda_2 = 4$ m^{-1} and $\lambda_3 = 80$ m^{-1}) and (b) square based columnar (long) block shapes ($\lambda_1 = \lambda_2 = 4$ m^{-1} and $\lambda_3 = 0.3$ m^{-1}).

or less for particularly rock masses including extremely closely spaced joints when compared with engineering dimension such as slope height. For this case, the value of AI'_{jd} may be expected to be reduced to zero for extremely closely (heavily) jointed rock mass.

(2) $TRQD_t$ as a directional parameter for defining the jointing degree is a powerful tool for the use of structural anisotropy classification from rock masses having extremely closely to extremely widely spaced joint sets.

(3) As a consequence of the hypothetical cases, it can be stated that the improved formulation of structural rock mass anisotropy index (AI'_{jd}) together with its classification has an application capacity to rock masses independent from spacing of joint sets.

4.2. Application to real cases

Application of the improved equation of AI'_{jd} to real cases with their presentations on structural anisotropy index classification chart is given herein. For this aim, two real cases were investigated in this study.

4.2.1. R-case-1

This case is assessment of stratified marl from Simav open pit borax mine in the western part of Turkey. The observations and measurements along the slope face were performed to determine the number of joint sets and their discontinuity spacing (Fig. 11).

The investigated slope face is located in the east side of an asymmetric synclinal within the geological stratification of rock mass. Therefore, orientation of stratification and joint sets may even change within the small distances. Thus, only the observed location was considered for identification of stratification and main joint sets with their orientations and mean discontinuity spacing values. The strike of slope face was N120°E and general orientation of stratification (J_1) was measured as 052°/48°. Thickness of stratification varies between a few centimeters to about a few tens of centimeters with an average value of about 5.2 cm ($\lambda_1 = 19.2$ m^{-1}) at this location. In addition to the stratification planes, two joint sets having general orientations of 195°/74° (J_2) and 098°/85° (J_3), with average joint spacing of 47 cm ($\lambda_2 = 2.1$ m^{-1}) and 48 cm ($\lambda_3 = 2.1$ m^{-1}), were identified, respectively. The schematic plan view of the identified discontinuity sets and view of slope faces are shown in Fig. 11.

In order to obtain $TRQD_{0.1,max}$, the values of $TRQD_{0.1}$ in 3D space were determined for every point representing a direction on equal-angle stereographic projection using Eq. (1), Eq. (3) and $t = 0.1$ m $TRQD_{0.1,max}$ was obtained as 98.3%. Similarly, the values of $TRQD_t$ in 3D space were also determined for every point (totally 360 points) representing a direction on equal-angle stereographic projection using Eqs. (1)–(3). The distribution counters of $TRQD_t$ and AI'_{jd} on equal-angle stereographic projection of stratified marl were given in Fig. 12. AI'_{jd} was determined as 46.6 using the values of $TRQD_{0.1,max}$, $TRQD_{t,max}$ and $TRQD_{0.1,min}$ in the improved formulation of structural anisotropy index given by Eq. (6). The value of $AI'_{jd} = 46.6$ is classified as "Moderate (M)" in the proposed classification.

However, as can be seen on the close view of the studied rock mass exposure in Fig. 11, the stratified marl should have a significant anisotropic mechanical behavior due to the stratification planes having high persistency. Up to this stage of the study, only the values of joint frequency for each identified joint set included in rock mass were considered with their orientations. However, in addition to the number of joint sets with their orientations,

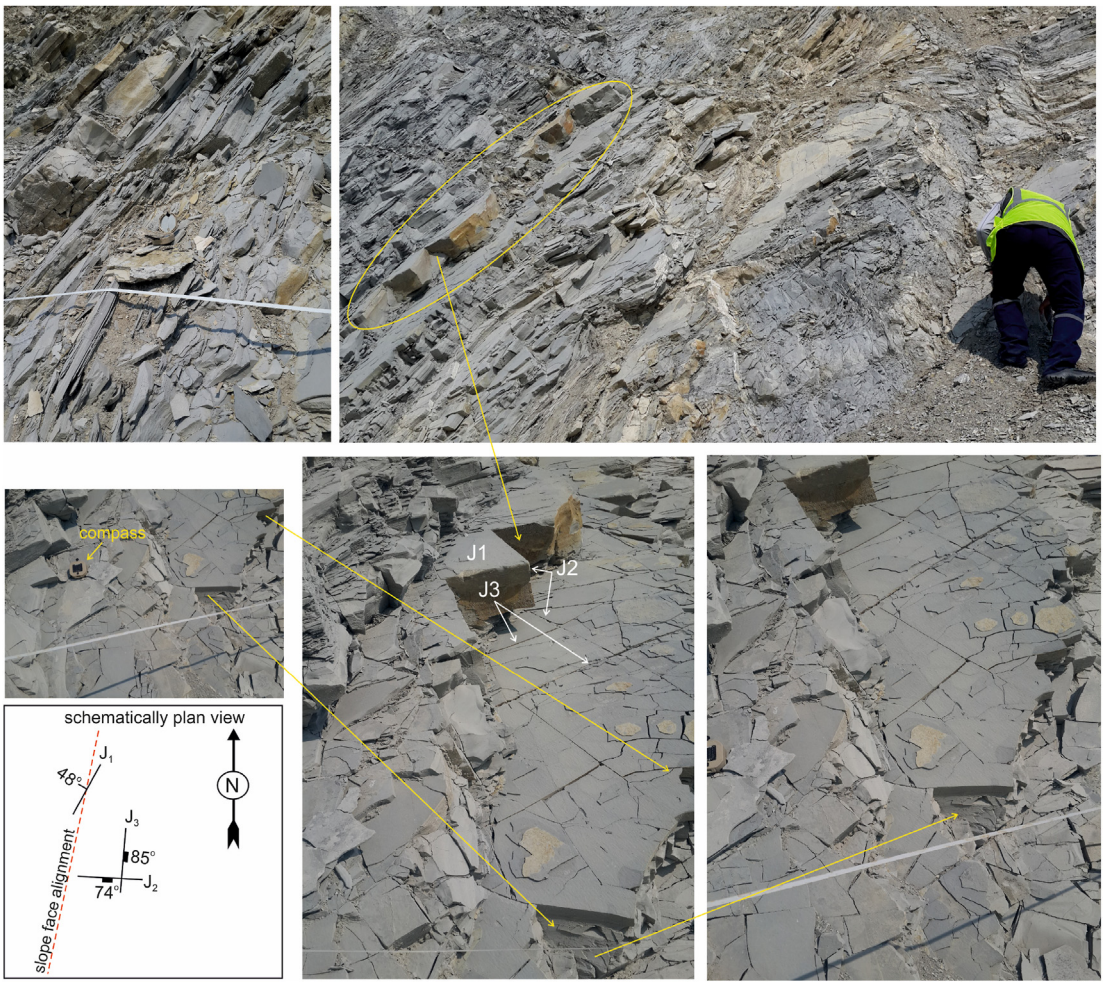

Fig. 11. The outcrop of the stratified rock mass studied and a schematic illustration about the measurements.

persistency of discontinuities has an important effect on the directional mechanical behavior of rock mass. The possible contribution of persistency of joints to the evaluation of structural anisotropy of rock masses was investigated in the next section after determination of AI'_{jd} with its current form given above.

4.2.2. R-case-2

The second real case study was investigated on columnar shaped basalts exposure in Bala region (in the close vicinity of Ankara) in Turkey (Fig. 13a). The basalt columns generally have a hexagonal cross-section perpendicular to the longest axis. The measurements of joint orientations in the columnar shaped basalts were performed together with the joint spacing. In addition to three joint sets formed hexagonal shaped sides of basalt columns, almost horizontally or low inclined joints were also measured (Fig. 13b). After the evaluation of the joint orientation measurements on equal-angle stereographic net, four joint sets were identified as J_1 (334°/31°), J_2 (208°/78°), J_3 (092°/83°) and J_4 (150°/70°) (Fig. 13c). Based on the statistical evaluations of the spacing of joint sets, the joint frequencies for each set were determined as $\lambda_1 = 1.308$ m^{-1}, $\lambda_2 = 2.116$ m^{-1}, $\lambda_3 = 2.232$ m^{-1} and $\lambda_4 = 2.087$ m^{-1} (Table 2).

Same procedure with R-case-2 was followed to obtain $TRQD_{0.1,max}$ and $TRQD_t$ distribution counters on equal-angle stereographic projection net of columnar basalt. While $TRQD_{0.1,max}$ was obtained as 99.1%, the distribution counters on equal-angle stereographic projection of columnar basalt are given in Fig. 14.

For the second real case, the values of $TRQD_{t,max}$ and $TRQD_{t,min}$ were determined as 99% and 90.2%, respectively. The improved structural anisotropy index (AI'_{jd}) was also determined as 8.8 and classified as "Very low (VL)" class in the proposed classification. Similar to stratified marl investigated in the first real case, side surfaces of basalt columns are the highest effective joints in the rock mass with their very high persistency (Fig. 13). It can be clearly said that anisotropic mechanical behavior should be expected high in terms of engineering significance for the columnar basalt. The main reason for this statement is the possible contribution of persistency of joints on the structural anisotropy of rock masses.

4.3. Introducing the effect of persistency of joints on structural anisotropy assessment

The new procedure proposed for the quantitative anisotropy assessment of rock mass given above produced meaningful results for hypothetical cases. For the hypothetical rock mass cases, persistency of joints was not considered. In other words, it was assumed that the hypothetical rock masses were formed by joint sets having the same persistency. However, it should be pointed out that the discontinuities with very high persistency have a significant importance on the anisotropic behavior of rock mass. Firstly, two real cases, one for the stratified marl and the other for the columnar basalt, were assessed to identify structural anisotropic behavior using AI'_{jd} and its classification without considering

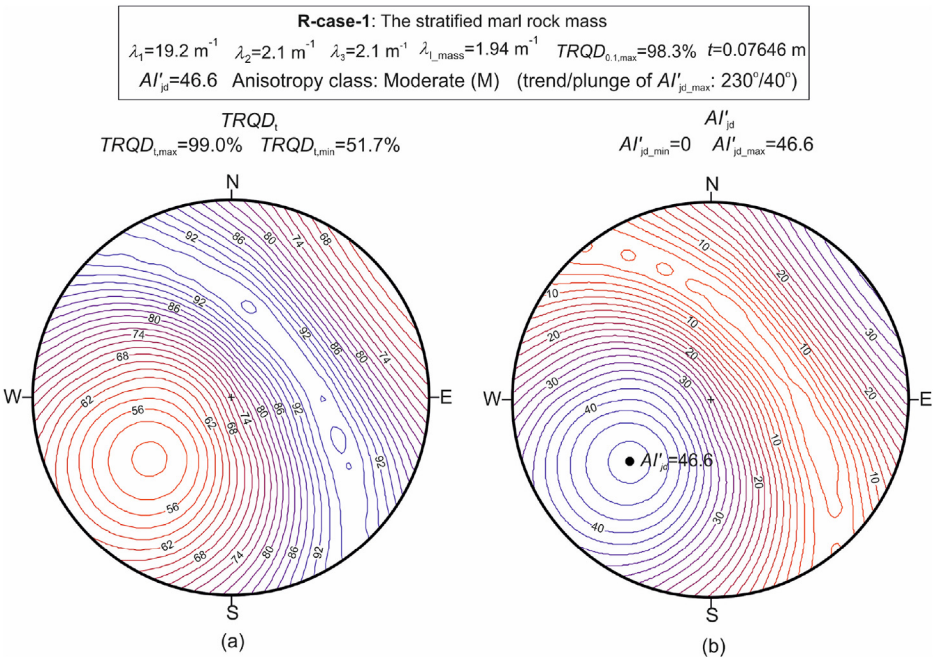

Fig. 12. (a) $TRQD_t$ and (b) AI'_{jd} counters on equal-angle stereographic projection for the stratified rock mass studied.

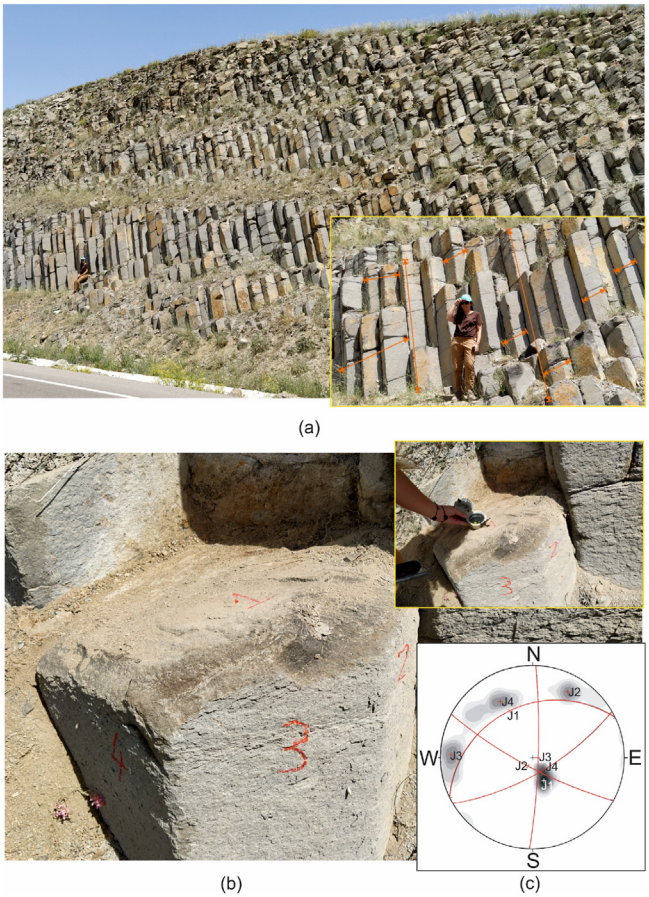

Fig. 13. (a) Columnar shaped basalt exposure studied as the second real case, (b) The close view of the measurement of orientation of joint surfaces of a basalt column, and (c) The joint orientation counters on equal-angle stereographic projection and the main orientation (trend/plunge) for each joint set.

persistency of the joints in the two rock masses. Although rock masses of both real cases have a significant structural anisotropic behavior, the values of AI'_{jd} were determined as 46.6 (moderate anisotropy) and 8.8 (very low anisotropy) for the stratified marl and the columnar basalt, respectively. One of the possible reasons for the conservative outputs may be related with the contribution of persistency of the joint sets. Both the hexagonal surfaces of basalt columns and the stratifications have very high persistency as can be clearly seen in Figs. 11 and 13. Therefore, the weighted contribution of the joint sets with their persistency was included to the improved anisotropy index formulation at this stage of the study. For the determination of the weighted contribution of each joint set, the use of the ratings suggested for the persistency of discontinuities in "geomechanical classification system", also known as *RMR* by Bieniawski (1989), was preferred (Table 3). As is well known, *RMR* has been one of the most commonly used and widely accepted geomechanical tools and classifications in rock mechanics.

Using the ratings given in *RMR*, the weight for persistency (w_p) of each joint set is defined by Eq. (7). In the relation, one added the value of R_{max} (= 6) to avoid possible undefined result due to dividing by zero (rating of very high persistency, $L > 20$ m).

$$w_p = \frac{(R_{max} + 1) - R}{R_{max} + 1} \tag{7}$$

The relation between average joint length (L) and the weight for the persistency (w_p) was investigated using average ratings and joint length of each class from very low to very high (Fig. 15). Following equation is obtained as the best fitting relation:

$$w_p = 0.156L^{0.6157} \tag{8}$$

where $L = 20$ m when L is larger than 20 m.

The weight factor for each joint set (w_f) is determined by the ratio of the maximum value of weight for persistency among the discontinuity sets ($w_{p,max}$) to the value of weight for persistency of

Table 2
Statistical evaluations of joint spacing for each joint set including their frequencies.

Joint No.	N	Spacing of joint set (cm)			Standard deviation (cm)	Frequency of joint set, λ (m^{-1})
		Minimum	Maximum	Mean		
J_1	25	20	159	76.48	33.46	1.308
J_2	8	38	55	47.25	6.32	2.116
J_3	10	41	50	44.80	3.12	2.232
J_4	11	39	66	47.91	7.94	2.087

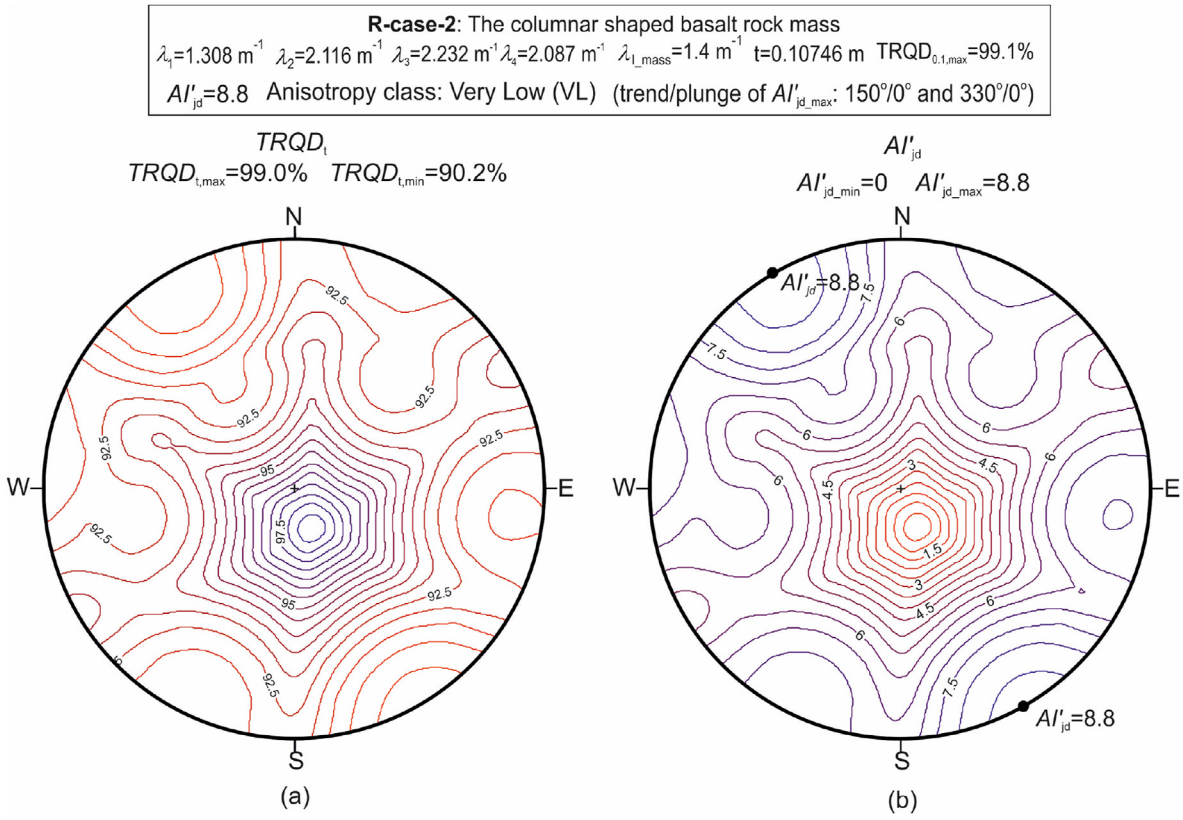

Fig. 14. (a) $TRQD_t$ and (b) AI'_{jd} curves on equal-angle stereographic projection for the columnar basalt studied.

Table 3
The definition, measurement and rating suggested for the persistency of discontinuities in *RMR* (from Bieniawski, 1989).

Definition	Measurement, L (m)	Rating, R
Very low	<1	6
Low	1–3	4
Moderate	3–10	2
High	10–20	1
Very high	>20	0

the related joint set ($w_{p,i}$) (Eq. (9a)). Finally, the weighted theoretical rock quality index ($W\text{-}TRQD_t$) and the weighted discontinuity frequency (λ_w) were redefined by Eqs. (9b) and (9c), respectively, by modifying the previous relations given in Eqs. (1) and (3). For certain, Eq. (6) can be used when there is no significant difference among the persistence of joint sets in rock mass.

However, when the significant difference among the persistency of joint sets exists, the improved anisotropy index for jointing degree (AI'_{jd}) relation given by Eq. (6) can be rearranged as W_TRQD_t by considering weighted assessment of frequency of joint sets (Eq. (10)). When the persistency of the joint sets is nearly equal to each other, the values of w_f for each discontinuity set will be obtained as almost equal to 1, which means that Eqs. (9b), (9c) and (9d) and 10 turn back to previously defined forms (Eqs. (1), (3) and (6)). This is why the hypothetical cases having no significant difference among the persistency of the joints surrounding the rock blocks have produced meaningful results.

$$w_f = \frac{w_{p,i}}{w_{p,max}} \tag{9a}$$

$$\lambda_w = \sum_{i=1}^{N} w_{f,i}\lambda_i \cos\theta_i \tag{9b}$$

$$t = 0.1484\left(\lambda_{w\_l\_mass}\right)^{-0.999} \tag{9c}$$

$$W\_TRQD_t(\%) = 100e^{-t\lambda_w}(t\lambda_w + 1) \tag{9d}$$

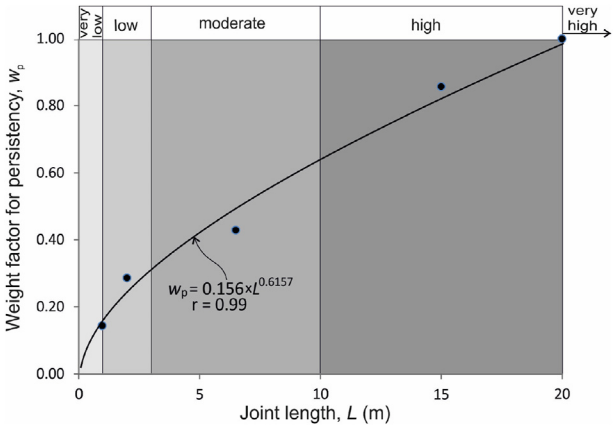

Fig. 15. The investigated relation between average joint length (L) and the weight factor for persistency (w_p).

$$W\_AI'_{jd} = \frac{W\_TRQD_{0.1,max}}{100}\left(W\_TRQD_{t,max} - W\_TRQD_{t,min}\right) \quad (10)$$

where $\lambda_{w\_l\_mass}$ is the lowest weighted frequency of joint sets in 3D rock mass medium, and $W\_AI'_{jd}$ is the weighted anisotropy index for jointing degree.

4.4. Application of weighted anisotropy index to real cases

As presented previously, the values of the improved anisotropy index for jointing degree (AI'_{jd}) were obtained as 46.6 and 8.8. According to these values, they were classified as "Moderate" and "Very low" anisotropic rock masses for the stratified marl and columnar basalt, respectively. However, two real cases should have significant anisotropic effect in terms of engineering behavior of the rock masses. Therefore, without contribution of persistency to structural anisotropy of rock mass, the obtained values can be evaluated as low capable of defining structural anisotropy. As can be seen in Fig. 11, the stratification planes with very high persistency which extends more than tens of meters (J_1) have more structural significance when compared with the other two joint sets (J_2 and J_3) with limited persistency within 3–10 m. Similarly, the side faces of the basal columns (J_2, J_3 and J_4) have very high persistency (>20 m) when compared with the persistency of the almost horizontal inclined joint set (from 0.5 m to 1.5 m) denoted by J_1 (Fig. 13).

Two real cases were also assessed by considering the contribution of persistency to the structural anisotropic behavior of rock masses. For this aim, weight of persistency for each joint set (w_p) was determined using Eq. (8) considering their persistency (equal to the values of average L for each joint set) in the rock mass. Then, the value of weight factor for each joint set (w_f) was calculated using Eq. (9a). The input parameters and the calculated values of w_p and w_f for each joint set in two real cases are summarized in Table 4.

Finally, the values of W_TRQD_t that consider contribution of persistency of the joint sets to structural anisotropy were calculated using Eqs. (9b), (9c) and (10) in 3D space for every point representing a direction by its trend and plunge on equal-angle stereographic projection. The counters of AI'_{jd} and $W\_AI'_{jd}$ on equal-angle stereographic projection for two real cases are shown in Fig. 16. The maximum and minimum values of AI'_{jd} and $W\_AI'_{jd}$ on equal-angle stereographic projection were set to 100 and 0, respectively, to satisfy the clear comparison of anisotropy

Table 4
The input parameters and the calculated values of w_p and w_f for each joint set in two real cases.

Rock type	Joint No.	Frequency of joint set, λ (m^{-1})	Persistency, L (m)	w_p (Eq. (8))	w_f (Eq. (9a))	$w_f\lambda_i$
Stratified marl	J_1	19.2	20 m (very high, >20 m)	0.99	1	19.2
	J_2	2.1	average 6.5 m (3–10 m)	0.494	0.498	1.027
	J_3	2.1	average 6.5 m (3–10 m)	0.494	0.498	1.027
Columnar basalt	J_1	1.308	average 0.75 m (0.5–1.5 m)	0.131	0.13	0.17
	J_2	2.116	20 m (very high, >20 m)	0.99	1	2.116
	J_3	2.232	20 m (very high, >20 m)	0.99	1	2.232
	J_4	2.087	20 m (very high, >20 m)	0.99	1	2.087

assessments based on AI'_{jd} and $W\_AI'_{jd}$. The values of $W\_AI'_{jd}$ for the stratified marl and columnar basalt were determined as 77.4 and 70.5, respectively, when the persistency of joint sets is taken into consideration. Two real rock masses having significant structural anisotropy were classified as "High" according to the proposed anisotropy classification. Therefore, it can be concluded that the weighted anisotropy index for jointing degree ($W\_AI'_{jd}$) has sufficient capability for assessment of structural anisotropy of rock masses together with the anisotropy classification proposed in this study.

5. Development of a structural anisotropy chart

To simplify application of the proposed method, the procedure for calculation of the weighted anisotropy index of jointing degree ($W\_AI'_{jd}$) is summarized in Fig. 17 for practitioner's consideration. Then, in addition to the proposal of the weighted anisotropy index for jointing degree, a structural anisotropy classification was developed based on the classes defined in RQD classification by Deere (1963). A graphical presentation for structural anisotropy index classification using two axes as "$W\_TRQD_{0.1,max}$" and "$\Delta W\_TRQD_t = W\_TRQD_{t,max} - W\_TRQD_{t,min}$" by considering boundary values of each class given in Fig. 3d is also produced (Fig. 18). The structural anisotropy assessments of hypothetical and real cases are plotted on the graphical presentation of the classification given in Fig. 18.

6. Conclusions

Structural anisotropic behavior may have significant importance in rock mass engineering projects depending on the number of sets, orientation, spacing and persistency of the discontinuities. For example, the strength and deformation properties of the stratified rock masses should have significant differences in parallel and perpendicular directions to the stratification planes. Similarly, the mechanical behavior of a rock mass composed of columnar block shapes will change depending on the applied stress direction on the rock mass.

RQD has been widely used as a 1D jointing degree property since it should be determined by measuring the core lengths obtained from drilling. However, to improve practical value of *RQD*, $TRQD_t$ introduced by Priest and Hudson (1976) was taken into consideration only when the statistical distribution of discontinuity spacing has a negative exponential distribution. *RQD*, as a directional property of a rock mass, has been used for

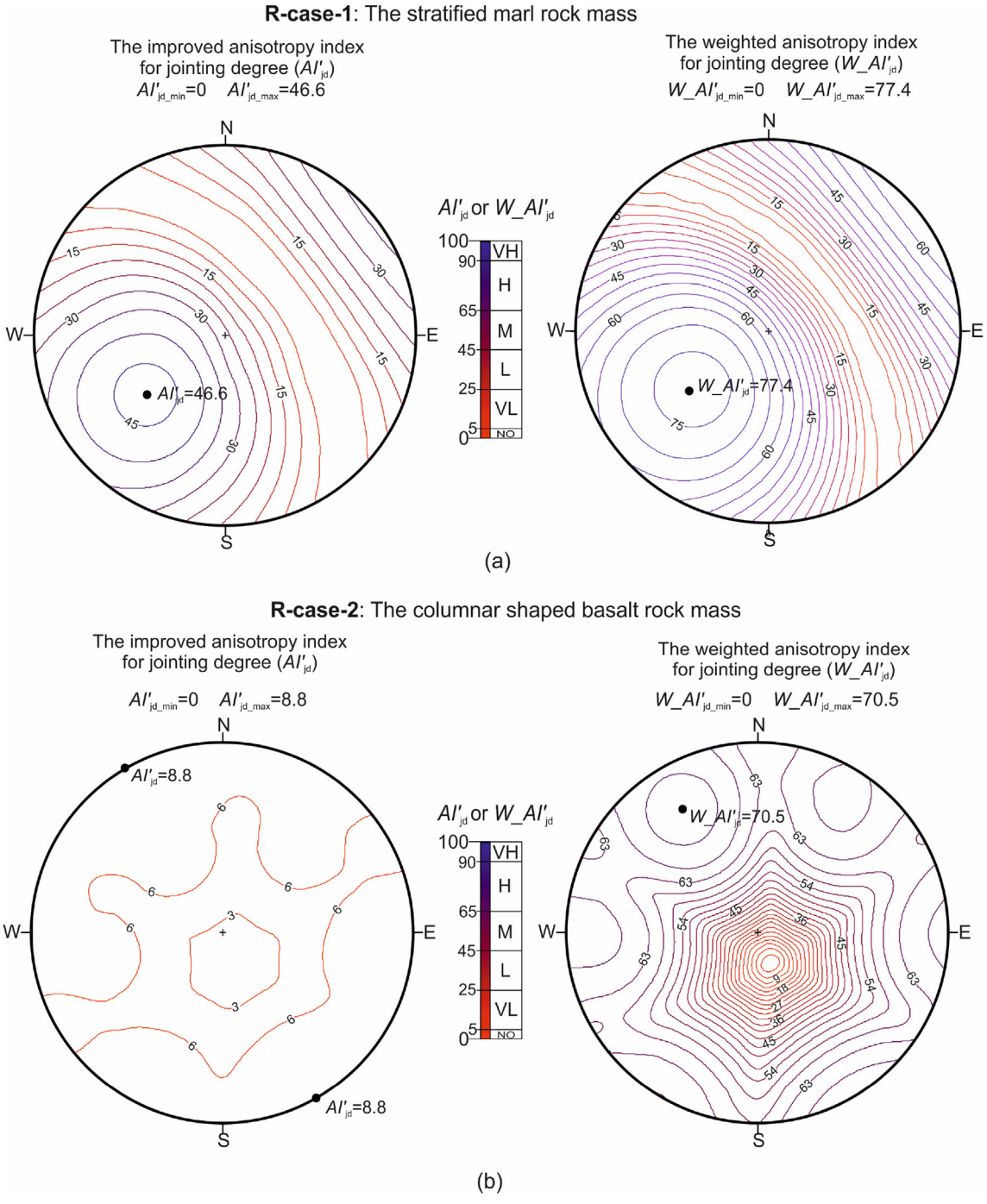

Fig. 16. The counters of AI'_{jd} and $W\_AI'_{jd}$ on equal-angle stereographic projection for two real cases: (a) R-case-1 and (b) R-case-2 within ranges between 0 and 100 as minimum and maximum, respectively.

defining the structural anisotropy. However, the use of *RQD* in rock mass has some limitations to define jointing degree for the rock masses composed of extremely closely spaced joints and for the rock mass including widely to extremely widely spaced joints due to the use of 0.1 m rock core length as a threshold in its conventional form.

In this study, by considering impressive recommendation by Priest (1993) for improving the sensitivity of *RQD* using different threshold levels of "*t*", the applicability of the formulation of anisotropy index for jointing degree proposed by Zheng et al. (2018) was improved. In addition, persistency of joint sets was also included in the anisotropy assessment of the jointed rock masses based on the rating of persistency in RMR_{89}.

Firstly, hypothetical rock masses were assessed using a novel approach to anisotropy classification and the calculation of the improved structural anisotropy index (AI'_{jd}). Then, the contribution of joint persistency to the structural anisotropy of the jointed rock masses was introduced to this new approach. The weighted improved structural anisotropy index ($W\_AI'_{jd}$) was assessed in two real cases.

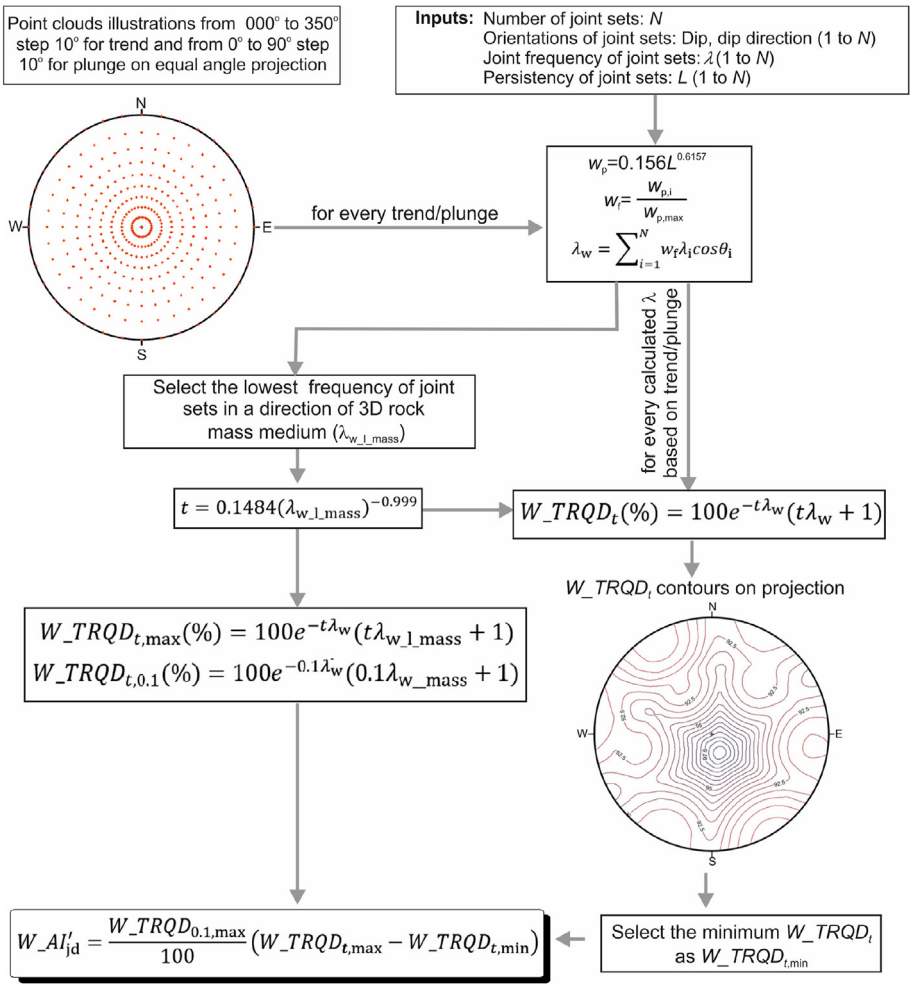

Fig. 17. The summary flowchart for determination of the weighted anisotropy index for jointing degree ($W\_AI'_{jd}$).

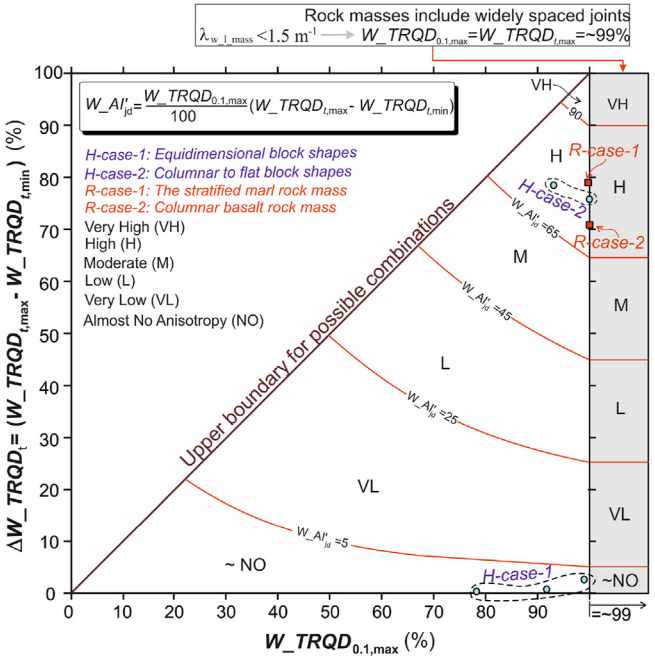

Fig. 18. Structural anisotropy chart based on the weighted structural anisotropy index classification proposed in this study and distribution of hypothetic and real rock mass cases.

It should be noted that the main focus of this study was the determination of degree of anisotropy of rock masses based on jointing degree, not to rate or classify the rock masses. Certainly, geomechanical rock mass classifications are of great importance in rock engineering, but the proposed methodology in this study can provide an input for such classifications. Furthermore, the proposed structural anisotropy evaluation procedure for jointed rock masses has an adaptation potential to the recent studies about automatic or semi-automatic determination of 3D joint distribution such as terrestrial LIDAR technique and UAV photogrammetry.

The repeated calculations are necessary on the spread Cartesian coordinate on equal-angle stereographic projection for application of the proposed formulations. Therefore, to increase practical value of the proposed formulations, a computer code was developed for free use of practitioners.

As a final conclusion, the applications of the weighted improved structural anisotropy index ($W\_AI'_{jd}$) to the hypothetical and real rock masses show that the proposed anisotropy classification has a sufficient capability of structural anisotropy assessment independent of scale of joint pattern.

Declaration of competing interest

The authors declare that they have no known competing financial interests or personal relationships that could have appeared to influence the work reported in this paper.

Acknowledgments

We appreciate the supports from the General Directorate of ETIMADEN enterprises during the field studies at Simav open pit mine. We would like to thank Prof. Yılmaz Özçelik and Mining Engineer Alper Entok for their assistance during the field studies. Finally, we also would like to thank the anonymous reviewers and the editor for the time and energy dedicated to this study for their valuable suggestions and comments.

References

Annels, A.E., Dominy, S.C., 2003. Core recovery and quality: important factors in mineral resource estimation. Appl. Earth Sci. 112, 305–312.
Barton, N., 2002. Some new Q-value correlations to assist in rock masses for the design of tunnel design. Int. J. Rock Mech. Min. Sci. 39, 185–216.
Bertuzzi, R., Douglas, K., Mostyn, G., 2016. Comparison of quantified and chart GSI for four rock masses. Eng. Geol. 202, 24–35.
Bieniawski, Z.T., 1989. Engineering Rock Mass Classifications. John Wiley and Sons.
Cheng, C., Chen, X., Zhang, S., 2016. Multi-peak deformation behavior of jointed rock mass under uniaxial compression: insight from particle flow modeling. Eng. Geol. 213, 25–45.
Choi, S.Y., Park, H.D., 2004. Variation of rock quality designation (RQD) with scanline orientation and length: a case study in Korea. Int. J. Rock Mech. Min. Sci. 41 (2), 207–221.
Coon, R.F., Merritt, A.H., 1970. Predicting in situ modulus of deformation using rock quality indexes. In: Determination of the in Situ Modulus of Deformation of Rock. ASTM International, Philadelphia, pp. 154–173.
Dearman, W.R., 1991. Engineering Geological Mapping. Butterworth–Heinemann, Oxford, UK.
Deere, D.U., 1963. Technical description of rock cores for engineering purpose. Rock Mech. Eng. Geol. 1 (1), 16–22.
Deere, D.U., 1968. Chapter 1, geologic considerations. In: Rock Mechanics in Engineering Practice. Wiley, pp. 1–20.
Deere, D.U., Deere, D.W., 1989. Rock Quality Designation (RQD) after Twenty Years. Technical Report. Department of the US Army Corps of Engineering, Washington, D.C., USA.
Deere, D.U., Hendron, A.J., Patton, F.D., Cording, E.J., 1967. Design of surface and near surface construction in rock. In: Proceedings of the 8th US Symposium on Rock Mechanics-Failure and Breakage of Rock. American Institute of Mining, Metallurgical and Petroleum Engineers, Inc., New York, USA, pp. 237–302.
Dinc, O.S., Sonmez, H., Tunusluoglu, C., Kasapoglu, K.E., 2011. A new general empirical approach for the prediction of rock mass strengths of soft to hard rock masses. Int. J. Rock Mech. Min. Sci. 48, 650–665.
Gardner, W.S., 1987. Design of drilled piers in the Atlantic Piedmont. In: Foundations and Excavations in Decomposed Rock of the Piedmont Province. American Society of Civil Engineers (ASCE), New York, USA, pp. 62–86.
Gokceoglu, C., Sonmez, H., Kayabasi, A., 2003. Predicting the deformation moduli of rock masses. Int. J. Rock Mech. Min. Sci. 40 (5), 701–710.
Hoek, E., Carter, T.G., Diederichs, M.S., 2013. Quantification of the geological strength index chart. In: Proceedings of the 47th US Rock Mechanics/geomechanics Symposium. American Rock Mechanics Association (ARMA). ARMA-2013-672.
Hudson, J.A., Priest, S.D., 1983. Discontinuity frequency in rock mass. Int. J. Rock Mech. Min. Sci. Geomech. Abstr. 20 (2), 75–89.
ISRM (International Society for Rock Mechanics), 1981. The ISRM Suggested Methods for Rock Characterization, Testing and Monitoring. Pergamon Press, Oxford, UK.
Jiang, Q., Feng, X.-T., Hatzor, Y.H., Hao, X.-J., Li, S.-J., 2014. Mechanical anisotropy of columnar jointed basalts: an example from the Baihetan hydropower station. Chin. Eng. Geol. 175 (10), 35–45.
Karzulovic, A., Goodman, R.E., 1985. Determination of principal fracture frequencies. Int. J. Rock Mech. Min. Sci. Geomech. Abstr. 22, 471–473.
Kayabasi, A., Gokceoglu, C., Ercanoglu, M., 2003. Estimating the deformation modulus of rock masses: a comparative study. Int. J. Rock Mech. Min. Sci. 40 (1), 55–63.
Kong, D., Wu, F., Saroglou, C., 2020. Automatic identification and characterization of discontinuities in rock masses from 3D point clouds. Eng. Geol. 265, 105442.
Kong, D., Saroglou, C., Wu, F., Sha, P., Li, B., 2021. Development and application of UAV-SfM photogrammetry for quantitative characterization of rock mass discontinuities. Int. J. Rock Mech. Min. Sci. 141, 104729.
Kulhawy, F.H., Goodman, R.E., 1987. Foundations in rock. In: Bell, F.G. (Ed.), Ground Engineer's Reference Book. Butterworths, London, UK.
Palmström, A., 1995. RMi - A Rock Mass Characterization System for Rock Engineering Purposes. PhD Thesis. University of Oslo.
Palmström, A., 2000. Recent developments in rock support estimates by the RMi. J. Rock Mech. Tunn. Technol. 6 (1), 1–19.
Palmström, A., 2005. Measurements of and correlations between block size and rock quality designation (RQD). Tunn. Undergr. Space Technol. 20, 362–377.
Priest, S.D., 1993. Discontinuity Analysis for Rock Engineering. Chapman & Hall, London, UK.
Priest, S.D., Hudson, J.A., 1976. Discontinuity spacings in rock. Int. J. Rock Mech. Min. Sci. Geomech. Abstr. 13 (5), 135–148.
Riquelme, A., Abellán, A., Tomás, R., 2015. Discontinuity spacing analysis in rock masses using 3D point clouds. Eng. Geol. 195, 185–195.
Saroglou, C., Qi, S., Guo, S., Wu, F., 2019. ARMR, a new classification system for the rating of anisotropic rock masses. Bull. Eng. Geol. Environ. 78, 3611–3626.
Sen, Z., 1984. RQD models and fracture spacing. J. Geotech. Eng. 110 (2), 203–216.
Sen, Z., Eissa, E.A., 1991. Volumetric rock quality designation. J. Geotech. Eng. 117 (9), 1331–1346.
Sen, Z., Sadagah, B.H., 2003. Modified rock mass classification system by continuous rating. Eng. Geol. 67 (3), 269–280.
Sow, D., Carvajal, C., Breul, P., Peyras, L., Rivard, P., Bacconnet, C., Ballivy, G., 2017. Modeling the spatial variability of the shear strength of discontinuities of rock masses: application to a dam rock mass. Eng. Geol. 220, 133–143.
Wang, P., Rena, F., Miao, S., Cai, M., Yang, T., 2017. Evaluation of the anisotropy and directionality of a jointed rock mass under numerical direct shear tests. Eng. Geol. 225, 29–41.
Wichmann, V., Strauhal, T., Fey, C., Perzlmaier, S., 2019. Derivation of space-resolved normal joint spacing and in situ block size distribution data from terrestrial LIDAR point clouds in a rugged Alpine relief (Kühtai, Austria). Bull. Eng. Geol. Environ. 78, 4465–4478.
Wu, F., Wu, J., Bao, H., Li, B., Shan, Z., Kong, D., 2021. Advances in statistical mechanics of rock masses and its engineering applications. J. Rock Mech. Geotech. Eng. 13 (1), 22–45.
Zhang, L., 2010. Estimating the strength of jointed rock masses. Rock Mech. Rock Eng. 43 (4), 391–402.
Zhang, L., Einstein, H.H., 2004. Using RQD to estimate the deformation modulus of rock masses. Int. J. Rock Mech. Min. Sci. 41 (2), 337–341.
Zheng, J., Zhao, Y., Lü, Q., Deng, J., Pan, X., Li, Y., 2016. A discussion on the adjustment parameters of the Slope Mass Rating (SMR) system for rock slopes. Eng. Geol. 206, 42–49.
Zheng, J., Yang, X., Lü, Q., Zhao, Y., Deng, J., Ding, Z., 2018. A new perspective for the directivity of Rock Quality Designation (RQD) and an anisotropy index of jointing degree for rock masses. Eng. Geol. 240, 81–94.
Zheng, J., Wang, X., Lü, Q., Liu, J., Guo, J., Liu, T., Deng, J., 2020. A contribution to relationship between volumetric joint count (J_v) and rock quality designation (RQD) in three-dimensional (3-D) space. Rock Mech. Rock Eng. 53, 1485–1494.

Dr. Harun Sonmez received his BSc and MSc degrees in Department of Geological Engineering from Hacettepe University, Turkey, in 1993 and 1996, respectively, and his PhD degree in the same department in 2001. Dr. Sonmez's special areas of research interest are rock mechanics, characterization of jointed rock masses, strength and deformation properties of rock materials, rock masses and block-in-matrix-rocks (bimrocks), stability of deep slopes and their design with remedial measures, monitoring of slope movements, mapping of landslides in terms of susceptibility, hazard and risk assessment, soil mechanics and earthquake triggered soil liquefaction and mapping strategies of soil liquefaction. Dr. Sonmez has also consulting expertise on engineering projects such as dam, tunnel and slope designs and constructions in Turkey and has been involved in many engineering geological projects such as open pit coal mining, landslide mapping, and mineral exploration. Numerous geotechnical softwares were developed by Dr. Sonmez during his research studies such as slope stability, kinematical analyses of rock slopes, artificial neural network, fractal dimension, liquefaction assessment, and monitoring of slopes.